Tetrahedron Letters 51 (2010) 4497–4500

Contents lists available at ScienceDirect

Tetrahedron Letters

journal homepage: www.elsevier.com/locate/tetlet

Tetrathiafulvalene hydrazone: efficient synthon for the synthesis of novel bidentate redox active ligands

Saleha Bakhta [a,b,c], Michel Guerro [a], Bellara Kolli [b], Frédéric Barrière [a], Thierry Roisnel [a], Dominique Lorcy [a,*]

[a] *Sciences Chimiques de Rennes, UMR 6226 CNRS-Université de Rennes 1, Campus de Beaulieu, Bât 10A, 35042 Rennes Cedex, France*
[b] *Laboratoire de Chimie Organique Université des Sciences et de la Technologie 'HouariBoumédienne', 16111 Alger, Algeria*
[c] *Centre de Recherche Scientifique et Technique en Analyse Physico-Chimiques (CRAPC) BP 248, Alger RP16004, Alger, Algeria*

ARTICLE INFO

Article history:
Received 28 May 2010
Revised 10 June 2010
Accepted 16 June 2010
Available online 20 June 2010

Keywords:
Tetrathiafulvalene
Redox active ligands
Redox behavior
Metal carbonyl complexes

ABSTRACT

The synthesis and the ability of TTF-hydrazone to act as a versatile precursor for the design of electroactive ligands are reported together with the chelating ability of these ligands through their $M(CO)_4$ complexes, (M = Mo, W).

Electroactive (P) and (N) ligands containing the redox active tetrathiafulvalene (TTF) unit have recently attracted attention in view of creating hybrid organic–inorganic multifunctional materials.[1] An interesting approach used for the synthesis of such electroactive ligands consists of introducing a reactive group on the preformed TTF core and subsequently linking a potentially coordinating moiety through this anchoring group. For instance, the introduction of a carboxaldehyde functionality on the TTF core allowed the grafting of a pyridine unit through either a conjugated ethylenic spacer group[2] or an imino bridge.[3] Among other reactive groups of interest to be grafted on TTF, hydrazones open many perspectives because a remaining free NH_2 can act as a novel anchoring group. However, among the large number of reported TTF derivatives, only a few examples of TTF carboxaldehydes have been condensed with hydrazine[4] and, to the best of our knowledge, the reaction toward TTF-hydrazones has not been reported yet. Hence, we sought to synthesize and investigate the potential of TTF-hydrazone derivatives with an intent to link other coordinating functionalities to the TTF core. Herein, we report the synthesis of the TTF-hydrazone synthon, followed by its condensation with either salicylidene or pyridyl groups, yielding, respectively, (N,O) and (N,N) bidentate TTF-based ligands. We further illustrate the chelating ability of the novel (N,N) electroactive ligand with the coordination of $M(CO)_4$ metal carbonyl fragments (M = Mo, W). The electrochemical properties of these ligands and metal complexes are also reported and discussed.

The target Me_3-TTF hydrazone **2** was prepared starting from Me_3-TTF carboxaldehyde **1**[5] as outlined in Scheme 1. The condensation of hydrazine to aldehyde **1** was carried out by simple mixing of a solution of TTF **1** with an excess of hydrazine monohydrate in acetonitrile at room temperature. According to this procedure, no product resulting from the biscondensation of TTF **1** with hydrazine was isolated but only TTF-hydrazone **2** was obtained. The remaining NH_2 group can then react with another aldehyde such as salicylaldehyde or 2-pyridine carboxaldehyde at room temperature to afford TTF ligands **3** and **4** respectively, as shown in Scheme 1.

Both TTF ligands **3** and **4** are deeply colored compounds and present similar UV-vis absorption spectra with a low-energy absorption band at $\lambda_{max} = 501$ nm ($\varepsilon = 9900\ L\ mol^{-1}\ cm^{-1}$) for **3** and $\lambda_{max} = 510$ nm ($\varepsilon = 5700\ L\ mol^{-1}\ cm^{-1}$) for **4**. This low energy absorption band is ascribed to an intramolecular charge transfer (ICT) between the TTF core and the electron accepting unit. The lower energy of the ICT band in **4** compared with the imino related compound **B** ($\lambda_{max} = 484$ nm)[3] is mainly due to the raising of the TTF-based HOMO in **4** due to the three donor methyl groups, as is also evident from the results of the theoretical calculations.

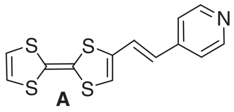

A
$\lambda_{max} = 444$ nm

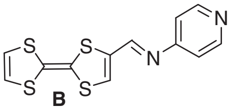

B
$\lambda_{max} = 484$ nm

Indeed, the DFT and TD-DFT calculations [GAUSSIAN03, B3LYP/6-31G**] carried out on **4** are in agreement with these assignments. As expected, the HOMO of **4** has a strong TTF character, while the LUMO

---

* Corresponding author. Fax: +33 2 23 23 67 38.
E-mail address: dominique.lorcy@univ-rennes1.fr (D. Lorcy).

0040-4039/$ - see front matter © 2010 Elsevier Ltd. All rights reserved.
doi:10.1016/j.tetlet.2010.06.088

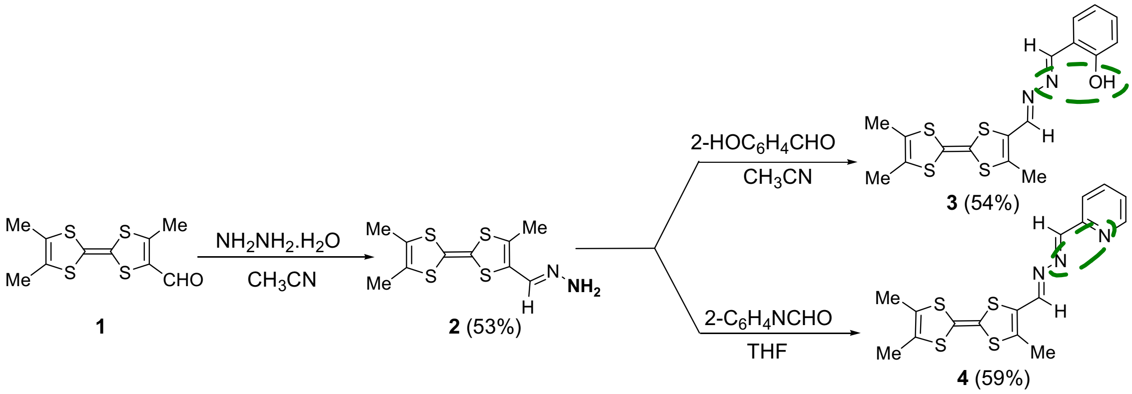

Scheme 1. Synthesis of bidentate (N,O) and (N,N) TTF-based ligands.

is mainly localized on the azinopyridine part (Fig. 1). The calculated HOMO–LUMO gap ΔE of **4** (ΔE = 2.44 eV, E_{HOMO} = −4.51 eV, E_{LUMO} = −2.07 eV) is smaller than that in **A** (ΔE = 2.84 eV, E_{HOMO} = −4.79 eV, E_{LUMO} = −1.95 eV) or in **B** (ΔE = 2.72 eV, E_{HOMO} = −4.83 eV, E_{LUMO} = −2.11 eV). The three methyl groups on the TTF in **4** raise the HOMO by 0.3 eV compared to **B** while the LUMO is essentially unaffected even if it is delocalized on a longer conjugated linker involving two additional atoms compared to **A** and **B**.

The electrochemical investigations carried out by cyclic voltammetry on **2**, **3**, and **4** give an insight on the effect of the potentially coordinating functionality on the redox properties of the TTF core (Table 1). All molecules display the expected two reversible monoelectronic processes corresponding to the reversible oxidation of the TTF to the cation radical and to the dication. The electronic effect of the hydrazine substituent in **2** is negligible when compared to simple trimethyl-TTF. In TTFs **3** and **4** however, the substituent grafted through the azino linker exerts an electron withdrawing effect and decreases the electronic density on the TTF core, as both oxidation potentials are shifted to higher values (+100 mV) compared to TTF **2**.

In order to form metal carbonyl complexes with TTF ligand **4**, we investigated its reactivity towards $Mo(CO)_6$. A solution of TTF **4** in dry and degassed toluene in the presence of one equivalent of $Mo(CO)_6$ was heated at reflux for 4 h (Scheme 2). Analysis of the reaction medium by ^1H NMR spectroscopy revealed a deshielding of the signals in the aromatic region, consistent with the coordination of the electroactive ligand **4** to the molybdenum center. After purification by chromatography on the silica gel column, a complex was isolated and analyzed by IR spectroscopy. The stretching absorption bands in the carbonyl region at 2014, 1904, 1878, 1827 cm^{-1} are characteristic of the $Mo(CO)_4$ fragment[6] leading to the [$Mo(CO)_4$(pyr-*N*,*N*-TTF)] formula for complex **5**. We also investigated the formation of the molybdenum TTF complex **5** through the addition of *cis*-$Mo(CO)_4$(piperidine)$_2$ instead of $Mo(CO)_6$ as it is known that the two piperidino labile ligands are easily displaced for the synthesis of $Mo(CO)_4$ complexes.[7] Thus, by simply mixing a stoichiometric amount of **4** and *cis*-$Mo(CO)_4(NHC_5H_{10})_2$ in CH_2Cl_2 at room temperature for 1 h, the TTF complex **5** was isolated. In these conditions, the reaction is faster than with $Mo(CO)_6$. Deep purple single crystals were obtained by the slow evaporation of a CH_2Cl_2 solution of **5** and X-ray crystal structure analysis (Fig. 2) confirmed the proposed structure with the molybdenum atom chelated by the azinopyridine group to form the five-membered metallacycle.[8] Within this constrained metallacycle, the N–Mo bond lengths are in the usual range with an N–Mo–N bite angle of 72.22°(5). The molybdenum center is coordinated in a distorted octahedral environment. The Mo–C bond lengths trans to the Mo–N (1.960(2) and 1.963(2) Å) are shorter than the two others Mo–C (2.043(2) and 2.065(2) Å) indicating a π-back metal to ligand donation.[9,10] The TTF moiety is almost planar with a C═C central bond length of 1.346(2) Å typical for a neutral TTF core. Moreover, the conjugated linker, the TTF moiety, and the pyridine group are coplanar.

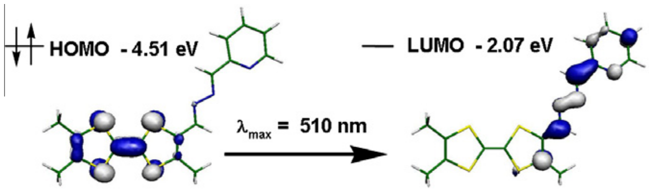

Figure 1. HOMO (left) and LUMO (right) of **4** calculated by DFT at B3LYP/6-31G**. Shown with a cut-off of 0.05 [e/bohr^3]$^{1/2}$.

Table 1
Oxidation potentials, *E* in *V* versus SCE, Pt working electrode with 0.1 M Bu_4NPF_6 in CH_2Cl_2

Compound	E^1 (TTF)	E_{pa} (Metal)	E^2 (TTF)
Me_3TTF	0.27		0.80
TTF **2**	0.29		0.80
TTF **3**	0.39		0.90
(pyr-*N*,*N*-TTF) **4**	0.39		0.91
cis-$Mo(CO)_4$(piperidine)$_2$		0.45	
cis-$W(CO)_4$(piperidine)$_2$		0.43	
cis-$Mo(CO)_4$(pyr-*N*,*N*-TTF) **5**	0.44	0.84	0.95
cis-$W(CO)_4$(pyr-*N*,*N*-TTF) **6**	0.45	0.78	0.86

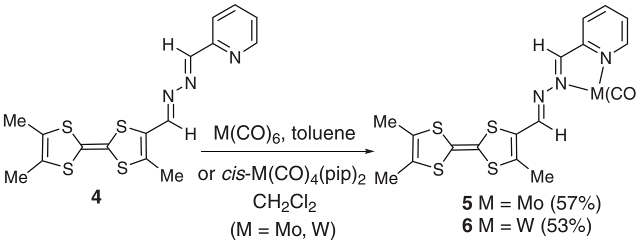

Scheme 2. Synthesis of metal carbonyl complexes of TTF-azinopyridine.

We further investigated the reactivity of the TTF ligand toward the analogous tungsten derivative, *cis*-$W(CO)_4(NHC_5H_{10})_2$ using a stoichiometric amount of both the reactants in CH_2Cl_2. In order to form the targeted complex **6**, the reaction mixture needs to be heated at reflux for 4 h to allow the substitution of the two piperidino ligands on the tungsten center by the TTF ligand **4**. The FT-IR spectrum of **6** exhibits four $\nu_{(CO)}$ at 2007, 1894, 1866, and 1804 cm^{-1} consistent with the presence of the $W(CO)_4$ fragment in an

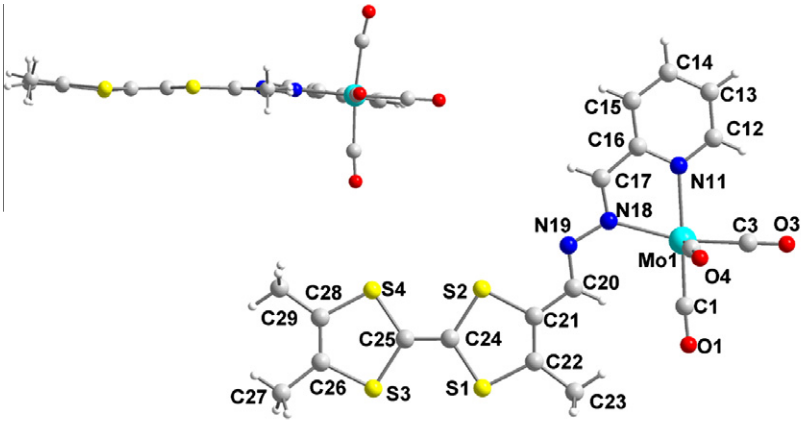

Figure 2. Molecular structure of *cis*-Mo$(CO)_4$(pyr-*N*,*N*-TTF) **5**.

octahedral environment with a (N,N) ligand in a cis arrangement. The X-ray crystal structure of *cis*-W$(CO)_4$(pyr-*N*,*N*-TTF)[8] has been determined and shows that **6** is isostructural to the Mo analog **5** with the following features: (i) a distorted octahedral environment around the tungsten atom with a bite angle N–W–N of 72.20(5)°, (ii) shorter W–C bond lengths trans to the W–N bond lengths than the cis ones (1.961(2) Å compared to 2.045(2) et 2.032(2) Å), (iii) coplanarity of the metallacycle and the TTF moiety, and (iv) a central C=C bond (1.349(3) Å) for the TTF characteristic of a neutral species. Both **5** and **6** present similar UV–vis absorption spectra with a low-energy absorption band at 564 nm ($\varepsilon = 4700\ \mathrm{L\ mol^{-1}\ cm^{-1}}$) for **5** and 551 nm ($\varepsilon = 2900\ \mathrm{L\ mol^{-1}\ cm^{-1}}$) for **6**. This low energy absorption band is ascribed to an ICT between the TTF moiety and the azinopyridine-metal unit behaving as a stronger electron acceptor than the azinopyridine one. DFT and TD-DFT calculations [GAUSSIAN03, B3LYP/LanL2DZ] carried out on **5** are consistent with these assignments and show that the HOMO of **5** has a strong TTF character, while the LUMO is mainly localized on the azinopyridine-metal part (Fig. 2). The calculated HOMO–LUMO gap ΔE ($\Delta E = 1.75$ eV, $E_{\mathrm{HOMO}} = -5.09$ eV, $E_{\mathrm{LUMO}} = -3.44$ eV) of **5** is smaller than that of the free ligand **4** ($\Delta E = 2.44$ eV).

The mutual influence of both the electrophores, that is, the metal and the TTF moieties, on the redox properties was studied by cyclic voltammetry. In CH_2Cl_2–[$n$$Bu_4N$][$PF_6$], three oxidation processes are observed for complexes **5** and **6**. The first process is reversible and corresponds to the oxidation of the TTF core to the cation radical while the second oxidation is irreversible and is attributed to the electrochemical response of the metal center. This assignment is consistent with the DFT calculations carried out on **5**$^{\cdot+}$, where the SOMO is found to have a strong metal contribution, (Fig. 3) The last reversible process is then associated with the reversible oxidation of the TTF cation radical into the dicationic species. The first oxidation potential of the TTF core is positively shifted by 50–60 mV in **5** and **6** ($E_1 = 0.44$ V for **5** and $E_1 = 0.45$ V for **6**) compared to the free ligand **4**. This shift quantifies the electron withdrawing effect exerted by the metal carbonyl fragment on the TTF core. The second and metal-based oxidation is irreversible for both metal complexes even at low temperatures ($E_{\mathrm{pa}} = 0.84$ V for **5** and $E_{\mathrm{pa}} = 0.78$ V for **6**). The oxidation peak potential of the metal center in **5** and **6** is also positively shifted (+390 mV for **5** and +350 mV for **6**) compared with *cis*-M$(CO)_4$(piperidine)$_2$ ($E_{\mathrm{pa}} = 0.45$ V for M = Mo and $E_{\mathrm{pa}} = 0.43$ V for M = W). This is ascribed to the presence of the positive charge of the oxidized TTF in the vicinity of the metal center.

Electrochemistry of **5** in CH_2Cl_2–Na[$B(C_6H_4(CF_3)_2)_4$] shows that the chemical reversibility of the second and metal-based oxidation may be restored even at moderate scan rates (Fig. 4). The electrochemical data in this poorly nucleophilic medium[11] indicate that the irreversibility of the metal based oxidation in CH_2Cl_2–[$n$$Bu_4N$][$PF_6$] probably involves the supporting salt anion. In the CH_2Cl_2—Na[$B(C_6H_4(CF_3)_2)_4$] medium, the redox potential of the second and third waves are shifted to even more anodic potentials because of the stronger electrostatic repulsion between the positive charges.[11]

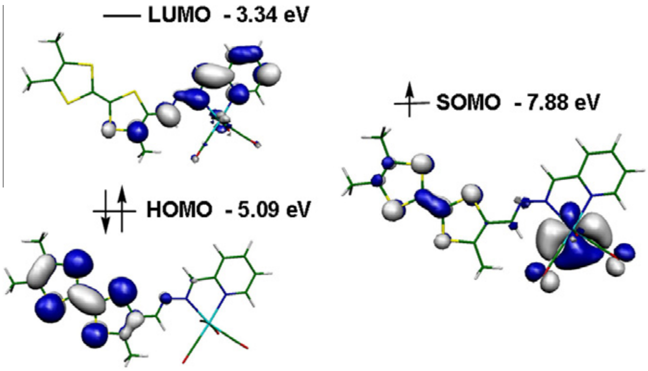

Figure 3. HOMO and LUMO of **5**, SOMO of **5**$^{\cdot+}$ calculated by DFT at B3LYP/LanL2DZ. Shown with a cut-off of 0.03 $[\mathrm{e/bohr^3}]^{1/2}$.

In summary, we have synthesized the electroactive synthon TTF-hydrazone, and showed that it is an excellent precursor for the design of two novel bidentate electroactive ligands with a non innocent azino linker: that is, it bridges the TTF core with either the phenol or pyridine moiety and brings about the bidentate (N,O or N,N) character. The chelating ability of the

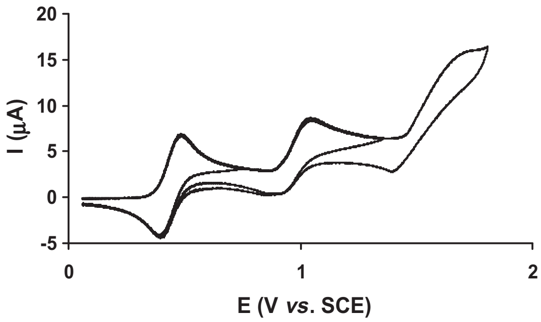

Figure 4. C.V. of **5** in CH_2Cl_2–Na[$B(C_6H_4(CF_3)_2)_4$] 0.02 M, $v = 100\ \mathrm{mV\ s^{-1}}$.

azinopyridine-based ligand was demonstrated through the formation of *cis*-$M(CO)_4$(pyr-*N*,*N*-TTF) complexes (M = Mo and W), whose electrochemical properties were also reported. We contend that this work opens novel opportunities in the design of bidentate TTF ligands and their metal complexes.[1]

Acknowledgment

The authors thank the CINES (Montpellier, France) for allocation of computing time.

Supplementary data

Supplementary data associated with this article can be found, in the online version, at doi:10.1016/j.tetlet.2010.06.088.

References and notes

1. Lorcy, D.; Bellec, N.; Fourmigué, M.; Avarvari, N.. *Coord. Chem. Rev.* **2009**, *253*, 1398–1438.
2. (a) Andreu, R.; Malfant, I.; Lacroix, P.; Cassoux, P. *Eur. J. Org. Chem.* **2000**, *3*, 737–741; (b) Xue, H.; Tang, X.-J.; Wu, L.-Z.; Zhang, L.-P.; Tung, C.-H. *J. Org. Chem.* **2005**, *70*, 9727–9734; (c) Benbellat, N.; Gavrilenko, K. S.; Le Gal, Y.; Cador, O.; Golhen, S.; Gouasmia, A.; Fabre, J.-M.; Ouahab, L. *Inorg. Chem.* **2006**, *45*, 10440–10442.
3. (a) Chahma, M.; Hassan, N.; Alberola, A.; Stoeckli-Evans, H.; Pilkington, M. *Inorg. Chem.* **2007**, *46*, 3807–3809; (b) Balandier, J.-Y.; Belyasmine, A.; Sallé, M. *Eur. J. Org. Chem.* **2008**, 269–276; (c) Cosquer, G.; Pointillard, F.; Le Gal, Y.; Golhen, S.; Cador, O.; Ouahab, L. *Dalton Trans.* **2009**, 3495–3502.
4. (a) Badri, M.; Majoral, J.-P.; Gonce, F.; Caminade, A.-M.; Salle, M.; Gorgues, A. *Tetrahedron Lett.* **1990**, *31*, 6343–6346; (b) Salle, M.; Gorgues, A.; Jubault, M.; Boubekeur, K.; Batail, P. *Tetrahedron* **1992**, *48*, 3081–3090.
5. Moore, A. J.; Bryce, M. R.; Batsanov, A. S.; Cole, J. C.; Howard, J. A. K. *Synthesis* **1995**, 675–682.
6. Kraihanzel, C. S.; Cotton, F. A. *Inorg. Chem.* **1963**, *2*, 533–540.
7. Darensbourg, D.; Kump, R. L. *Inorg. Chem.* **1978**, *17*, 2680–2682.
8. The X-ray crystallographic data for **5** and **6** have been deposited, as supplementary publication number CCDC 769485 and CCDC 769486, respectively at the Cambridge Crystallographic Data. Copies of the data can be obtained free of charge from the CCDC, 12 Union Road, Cambridge CB2 1EZ, UK; e-mail: deposit@ccdc.cam.ac.uk.
9. Cotton, F. A.; Darensbourg, D.; Klein, S.; Kolthammer, B. *Inorg. Chem.* **1982**, *21*, 1651–1655.
10. Riobé, F.; Avarvari, N. *Chem. Commun.* **2009**, 3753–3755.
11. (a) Barrière, F.; Geiger, W. E. *J. Am. Chem. Soc.* **2006**, *128*, 3980–3989; (b) Geiger, W. E.; Barrière, F. *Acc. Chem. Res.* **2010**. doi:10.1021/ar1000023; (c) Barrière, F.; LeSuer, R. J.; Geiger, W. E. Electrochemical Advances Using Fluoroarylborate Anion Supporting Electrolytes. In *Trends in Molecular Electrochemistry*; Pombeiro, A. J. L., Amatore, C., Eds.; Fontis Media, Marcel Dekker, 2004; pp 413–444. Chapter 13.